Measurement of the CP Violation Parameter $\sin 2\phi_1$ in B_d^0 Meson Decays

A. Abashian,[44] K. Abe,[8] K. Abe,[36] I. Adachi,[8] Byoung Sup Ahn,[14] H. Aihara,[37] M. Akatsu,[19] G. Alimonti,[7] K. Aoki,[8] K. Asai,[20] M. Asai,[9] Y. Asano,[42] T. Aso,[41] V. Aulchenko,[2] T. Aushev,[12] A. M. Bakich,[33] E. Banas,[15] S. Behari,[8] P. K. Behera,[43] D. Beiline,[2] A. Bondar,[2] A. Bozek,[15] T. E. Browder,[7] B. C. K. Casey,[7] P. Chang,[23] Y. Chao,[23] B. G. Cheon,[32] S.-K. Choi,[6] Y. Choi,[32] Y. Doi,[8] J. Dragic,[17] A. Drutskoy,[12] S. Eidelman,[2] Y. Enari,[19] R. Enomoto,[8,10] C. W. Everton,[17] F. Fang,[7] H. Fujii,[8] K. Fujimoto,[19] Y. Fujita,[8] C. Fukunaga,[39] M. Fukushima,[10] A. Garmash,[2,8] A. Gordon,[17] K. Gotow,[44] H. Guler,[7] R. Guo,[21] J. Haba,[8] T. Haji,[37] H. Hamasaki,[8] K. Hanagaki,[29] F. Handa,[36] K. Hara,[27] T. Hara,[27] T. Haruyama,[8] N. C. Hastings,[17] K. Hayashi,[8] H. Hayashii,[20] M. Hazumi,[27] E. M. Heenan,[17] Y. Higashi,[8] Y. Higashino,[19] I. Higuchi,[36] T. Higuchi,[37] T. Hirai,[38] H. Hirano,[40] M. Hirose,[19] T. Hojo,[27] Y. Hoshi,[35] K. Hoshina,[40] W.-S. Hou,[23] S.-C. Hsu,[23] H.-C. Huang,[23] Y.-C. Huang,[21] S. Ichizawa,[38] Y. Igarashi,[8] T. Iijima,[8] H. Ikeda,[8] K. Ikeda,[20] K. Inami,[19] Y. Inoue,[26] A. Ishikawa,[19] H. Ishino,[38] R. Itoh,[8] G. Iwai,[25] M. Iwai,[8] M. Iwamoto,[3] H. Iwasaki,[8] Y. Iwasaki,[8] D. J. Jackson,[27] P. Jalocha,[15] H. K. Jang,[31] M. Jones,[7] R. Kagan,[12] H. Kakuno,[38] J. Kaneko,[38] J. H. Kang,[45] J. S. Kang,[14] P. Kapusta,[15] K. Kasami,[8] N. Katayama,[8] H. Kawai,[3] H. Kawai,[37] M. Kawai,[8] N. Kawamura,[1] T. Kawasaki,[25] H. Kichimi,[8] D. W. Kim,[32] Heejong Kim,[45] H. J. Kim,[45] Hyunwoo Kim,[14] S. K. Kim,[31] K. Kinoshita,[5] S. Kobayashi,[30] S. Koike,[8] S. Koishi,[38] Y. Kondo,[8] H. Konishi,[40] K. Korotushenko,[29] P. Krokovny,[2] R. Kulasiri,[5] S. Kumar,[28] T. Kuniya,[30] E. Kurihara,[3] A. Kuzmin,[2] Y.-J. Kwon,[45] M. H. Lee,[8] S. H. Lee,[31] C. Leonidopoulos,[29] H.-B. Li,[11] R.-S. Lu,[23] Y. Makida,[8] A. Manabe,[8] D. Marlow,[29] T. Matsubara,[37] T. Matsuda,[8] S. Matsui,[19] S. Matsumoto,[4] T. Matsumoto,[19] Y. Mikami,[36] K. Misono,[19] K. Miyabayashi,[20] H. Miyake,[27] H. Miyata,[25] L. C. Moffitt,[17] A. Mohapatra,[43] G. R. Moloney,[17] G. F. Moorhead,[17] N. Morgan,[44] S. Mori,[42] T. Mori,[4] A. Murakami,[30] T. Nagamine,[36] Y. Nagasaka,[18] Y. Nagashima,[27] T. Nakadaira,[37] T. Nakamura,[38] E. Nakano,[26] M. Nakao,[8] H. Nakazawa,[4] J. W. Nam,[32] S. Narita,[36] Z. Natkaniec,[15] K. Neichi,[35] S. Nishida,[16] O. Nitoh,[40] S. Noguchi,[20] T. Nozaki,[8] S. Ogawa,[34] T. Ohshima,[19] Y. Ohshima,[38] T. Okabe,[19] T. Okazaki,[20] S. Okuno,[13] S. L. Olsen,[7] W. Ostrowicz,[15] H. Ozaki,[8] P. Pakhlov,[12] H. Palka,[15] C. S. Park,[31] C. W. Park,[14] H. Park,[14] L. S. Peak,[33] M. Peters,[7] L. E. Piilonen,[44] E. Prebys,[29] J. L. Rodriguez,[7] N. Root,[2] M. Rozanska,[15] K. Rybicki,[15] J. Ryuko,[27] H. Sagawa,[8] S. Saitoh,[3] Y. Sakai,[8] H. Sakamoto,[16] H. Sakaue,[26] M. Satapathy,[43] N. Sato,[8] A. Satpathy,[8,5] S. Schrenk,[5] S. Semenov,[12] Y. Settai,[4] M. E. Sevior,[17] H. Shibuya,[34] B. Shwartz,[2] A. Sidorov,[2] V. Sidorov,[2] J. B. Singh,[28] S. Stanič,[42] A. Sugi,[19] A. Sugiyama,[19] K. Sumisawa,[27] T. Sumiyoshi,[8] J. Suzuki,[8] J.-I. Suzuki,[8] K. Suzuki,[3] S. Suzuki,[19] S. Y. Suzuki,[8] S. K. Swain,[7] H. Tajima,[37] T. Takahashi,[26] F. Takasaki,[8] M. Takita,[27] K. Tamai,[8] N. Tamura,[25] J. Tanaka,[37] M. Tanaka,[8] Y. Tanaka,[18] G. N. Taylor,[17] Y. Teramoto,[26] M. Tomoto,[19] T. Tomura,[37] S. N. Tovey,[17] K. Trabelsi,[7] T. Tsuboyama,[8] Y. Tsujita,[42] T. Tsukamoto,[8] T. Tsukamoto,[30] S. Uehara,[8] K. Ueno,[23] N. Ujiie,[8] Y. Unno,[3] S. Uno,[8] Y. Ushiroda,[16] Y. Usov,[2] S. E. Vahsen,[29] G. Varner,[7] K. E. Varvell,[33] C. C. Wang,[23] C. H. Wang,[22] M.-Z. Wang,[23] T. J. Wang,[11] Y. Watanabe,[38] E. Won,[31] B. D. Yabsley,[8] Y. Yamada,[8] M. Yamaga,[36] A. Yamaguchi,[36] H. Yamaguchi,[8] H. Yamamoto,[7] T. Yamanaka,[27] H. Yamaoka,[8] Y. Yamaoka,[8] Y. Yamashita,[24] M. Yamauchi,[8] S. Yanaka,[38] M. Yokoyama,[37] K. Yoshida,[19] Y. Yusa,[36] H. Yuta,[1] C. C. Zhang,[11] H. W. Zhao,[8] J. Zhang,[42] Y. Zheng,[7] V. Zhilich,[2] and D. Žontar[42]

[1]*Aomori University, Aomori*
[2]*Budker Institute of Nuclear Physics, Novosibirsk*
[3]*Chiba University, Chiba*
[4]*Chuo University, Tokyo*
[5]*University of Cincinnati, Cincinnati, Ohio*
[6]*Gyeongsang National University, Chinju*
[7]*University of Hawaii, Honolulu, Hawaii*
[8]*High Energy Accelerator Research Organization (KEK), Tsukuba*
[9]*Hiroshima Institute of Technology, Hiroshima*
[10]*Institute for Cosmic Ray Research, University of Tokyo, Tokyo*
[11]*Institute of High Energy Physics, Chinese Academy of Sciences, Beijing*
[12]*Institute for Theoretical and Experimental Physics, Moscow*
[13]*Kanagawa University, Yokohama*
[14]*Korea University, Seoul*
[15]*H. Niewodniczanski Institute of Nuclear Physics, Krakow*
[16]*Kyoto University, Kyoto*
[17]*University of Melbourne, Victoria*

[18]*Nagasaki Institute of Applied Science, Nagasaki*
[19]*Nagoya University, Nagoya*
[20]*Nara Women's University, Nara*
[21]*National Kaohsiung Normal University, Kaohsiung*
[22]*National Lien-Ho Institute of Technology, Miao Li*
[23]*National Taiwan University, Taipei*
[24]*Nihon Dental College, Niigata*
[25]*Niigata University, Niigata*
[26]*Osaka City University, Osaka*
[27]*Osaka University, Osaka*
[28]*Panjab University, Chandigarh*
[29]*Princeton University, Princeton, New Jersey*
[30]*Saga University, Saga*
[31]*Seoul National University, Seoul*
[32]*Sungkyunkwan University, Suwon*
[33]*University of Sydney, Sydney NSW*
[34]*Toho University, Funabashi*
[35]*Tohoku Gakuin University, Tagajo*
[36]*Tohoku University, Sendai*
[37]*University of Tokyo, Tokyo*
[38]*Tokyo Institute of Technology, Tokyo*
[39]*Tokyo Metropolitan University, Tokyo*
[40]*Tokyo University of Agriculture and Technology, Tokyo*
[41]*Toyama National College of Maritime Technology, Toyama*
[42]*University of Tsukuba, Tsukuba*
[43]*Utkal University, Bhubaneswer*
[44]*Virginia Polytechnic Institute and State University, Blacksburg, Virginia*
[45]*Yonsei University, Seoul*
(Received 9 February 2001)

We present a measurement of the standard model CP violation parameter $\sin 2\phi_1$ (also known as $\sin 2\beta$) based on a 10.5 fb^{-1} data sample collected at the $\Upsilon(4S)$ resonance with the Belle detector at the KEKB asymmetric e^+e^- collider. One neutral B meson is reconstructed in the $J/\psi K_S$, $\psi(2S)K_S$, $\chi_{c1}K_S$, $\eta_c K_S$, $J/\psi K_L$, or $J/\psi\pi^0$ CP-eigenstate decay channel and the flavor of the accompanying B meson is identified from its charged particle decay products. From the asymmetry in the distribution of the time interval between the two B-meson decay points, we determine $\sin 2\phi_1 = 0.58^{+0.32}_{-0.34}(\text{stat})^{+0.09}_{-0.10}(\text{syst})$.

DOI: 10.1103/PhysRevLett.86.2509 PACS numbers: 11.30.Er, 12.15.Hh, 13.25.Hw

In the standard model (SM), CP violation arises from a complex phase in the Cabibbo-Kobayashi-Maskawa (CKM) quark mixing matrix [1]. In particular, the SM predicts a CP violating asymmetry in the time-dependent rates for B_d^0 and $\overline{B}_d^0$ decays to a common CP eigenstate, f_{CP}, without theoretical ambiguity due to strong interactions [2]:

$$\begin{aligned} A(t) &\equiv \frac{\Gamma(\overline{B}_d^0 \to f_{CP}) - \Gamma(B_d^0 \to f_{CP})}{\Gamma(\overline{B}_d^0 \to f_{CP}) + \Gamma(B_d^0 \to f_{CP})} \\ &= -\xi_f \sin 2\phi_1 \sin\Delta m_d t\,, \end{aligned}$$

where $\Gamma[\overline{B}_d^0(B_d^0) \to f_{CP}]$ is the decay rate for a $\overline{B}_d^0$ (B_d^0) to f_{CP} at a proper time t after production, ξ_f is the CP eigenvalue of f_{CP}, Δm_d is the mass difference between the two B_d^0 mass eigenstates, and ϕ_1 is one of the three internal angles of the CKM unitarity triangle, defined as $\phi_1 \equiv \pi - \arg(\frac{-V_{tb}^* V_{td}}{-V_{cb}^* V_{cd}})$ [3].

In this Letter, we report a measurement of $\sin 2\phi_1$ using $B_d^0\overline{B}_d^0$ meson pairs produced at the $\Upsilon(4S)$ resonance, where the two mesons remain in a coherent p-wave state until one of them decays. The decay of one of the B mesons to a self-tagging state, f_{tag}, i.e., a final state that distinguishes between B_d^0 and $\overline{B}_d^0$, at time t_{tag} projects the accompanying meson onto the opposite b-flavor at that time; this meson decays to f_{CP} at time t_{CP}. The CP violation manifests itself as an asymmetry $A(\Delta t)$, where Δt is the proper time interval $\Delta t \equiv t_{CP} - t_{\text{tag}}$.

The data sample corresponds to an integrated luminosity of 10.5 fb^{-1} collected with the Belle detector [4] at the KEKB asymmetric e^+e^- (3.5 on 8 GeV) collider [5]. At KEKB, the $\Upsilon(4S)$ is produced with a Lorentz boost of $\beta\gamma = 0.425$ along the electron beam direction (z direction). Because the B_d^0 and $\overline{B}_d^0$ mesons are nearly at rest in the $\Upsilon(4S)$ center of mass system (cms), Δt can be determined from the z distance between the f_{CP} and f_{tag} decay vertices, $\Delta z \equiv z_{CP} - z_{\text{tag}}$, as $\Delta t \simeq \Delta z/\beta\gamma c$.

The Belle detector consists of a 3-layer silicon vertex detector (SVD), a 50-layer central drift chamber (CDC), an array of 1188 aerogel Čerenkov counters (ACC), 128 time-of-flight (TOF) scintillation counters, and an electromagnetic calorimeter containing 8736 CsI(Tl) crystals (ECL) all located inside a 3.4-m-diameter superconducting solenoid that generates a 1.5 T magnetic field. The transverse momentum resolution for charged tracks is $(\sigma_{p_t}/p_t)^2 = (0.0019p_t)^2 + (0.0034)^2$, where p_t is in GeV/c, and the impact parameter resolutions for $p = 1$ GeV/c tracks at normal incidence are $\sigma_{r\phi} \simeq \sigma_z = 55$ μm. Specific ionization (dE/dx) measurements in the CDC ($\sigma_{dE/dx} =$ 6.9% for minimum ionizing pions), TOF flight-time measurements ($\sigma_{\rm TOF} = 95$ ps), and the response of the ACC provide $K^\pm$ identification with an efficiency of ~85% and a charged pion fake rate of ~10% for all momenta up to 3.5 GeV/c. Photons are identified as ECL showers that have a minimum energy of 20 MeV and are not matched to a charged track. The photon energy resolution is $(\sigma_E/E)^2 = (0.013)^2 + (0.0007/E)^2 + (0.008/E^{1/4})^2$, where E is in GeV. Electron identification is based on a combination of CDC dE/dx information, the ACC response, and the position relative to the extrapolated track, shape, and energy deposit of the associated ECL shower. The efficiency is greater than 90% and the hadron fake rate is ~0.3% for $p > 1$ GeV/c. An iron flux-return yoke outside the solenoid, comprised of 14 layers of 4.7-cm-thick iron plates interleaved with a system of resistive plate counters (KLM), provides muon identification with an efficiency greater than 90% and a hadron fake rate less than 2% for $p > 1$ GeV/c. The KLM is used in conjunction with the ECL to detect K_L mesons; the angular resolution of the K_L direction measurement ranges between 1.5° and 3°.

We reconstruct B_d^0 decays to the following CP eigenstates: $J/\psi K_S$, $\psi(2S)K_S$, $\chi_{c1}K_S$, $\eta_c K_S$ for $\xi_f = -1$ and $J/\psi\pi^0$, $J/\psi K_L$ for $\xi_f = +1$. The J/ψ and $\psi(2S)$ mesons are reconstructed via their decays to $\ell^+\ell^-$ ($\ell = \mu, e$). The $\psi(2S)$ is also reconstructed via its $J/\psi\pi^+\pi^-$ decay, the χ_{c1} via its $J/\psi\gamma$ decay, and the η_c via its $K^+K^-\pi^0$ and $K_S(\pi^+\pi^-)K^-\pi^+$ [6] decays.

For J/ψ and $\psi(2S) \to \ell^+\ell^-$ decays, we use oppositely charged track pairs, where both tracks are positively identified as leptons. For the $B_d^0 \to J/\psi K_S(\pi^+\pi^-)$ mode, the requirement for *one* of the tracks is relaxed: a track with an ECL energy deposit consistent with a minimum ionizing particle is accepted as a muon and a track that satisfies either the dE/dx or the ECL shower energy requirements as an electron. For e^+e^- pairs, we include the four-momentum of every photon detected within 0.05 rad of the original e^+ or e^- direction in the invariant mass calculation. Nevertheless a radiative tail remains and we accept pairs in the asymmetric invariant mass interval between -12.5σ and $+3\sigma$ of $M_{J/\psi}$ or $M_{\psi(2S)}$, where $\sigma =$ 12 MeV/c^2 is the mass resolution. The $\mu^+\mu^-$ radiative tail is smaller; we select pairs within -5σ and $+3\sigma$ of $M_{J/\psi}$ or $M_{\psi(2S)}$. Candidate $K_S \to \pi^+\pi^-$ decays are oppositely charged track pairs that have an invariant mass within $\pm 4\sigma$ of the K^0 mass ($\sigma \simeq 4$ MeV/c^2). For the $J/\psi K_S$ final state, $K_S \to \pi^0\pi^0$ decays are also used. For $\pi^0\pi^0$ candidates, we try all combinations where there are two $\gamma\gamma$ pairs with an invariant mass between 80 and 150 MeV/c^2, assuming they originate from the center of the run-dependent average interaction point (IP). We minimize the sum of the χ^2 values from constrained fits of each pair to the π^0 mass with γ directions determined by varying the decay point along the K_S flight path, which is taken as the line from the IP to the energy-weighted center of the four showers. We select combinations with a $\pi^0\pi^0$ invariant mass within $\sim\pm 3\sigma$ of M_{K^0}, where $\sigma \simeq 9.3$ MeV/c^2. For the $J/\psi\pi^0$ mode, we use a minimum γ energy of 100 MeV and select $\gamma\gamma$ pairs with an invariant mass within $\pm 3\sigma$ of M_{π^0}, where $\sigma \simeq 4.9$ MeV/c^2.

We isolate reconstructed B-meson decays using the energy difference $\Delta E \equiv E_B^{\rm cms} - E_{\rm beam}^{\rm cms}$ and the beam-energy constrained mass $M_{bc} \equiv \sqrt{(E_{\rm beam}^{\rm cms})^2 - (p_B^{\rm cms})^2}$, where $E_{\rm beam}^{\rm cms}$ is the cms beam energy, and $E_B^{\rm cms}$ and $p_B^{\rm cms}$ are the cms energy and momentum of the B candidate. Figure 1 shows the M_{bc} distribution for all channels combined (other than $J/\psi K_L$) after a ΔE selection that varies from ± 25 to ± 100 MeV (corresponding to $\sim\pm 3\sigma$), depending on the mode. The B-meson signal region is defined as $5.270 < M_{bc} < 5.290$ GeV/c^2; the M_{bc} resolution is 3.0 MeV/c^2. Table I lists the numbers of observed events ($N_{\rm ev}$) and the background ($N_{\rm bkgd}$) determined by extrapolating the event rate in the nonsignal ΔE vs M_{bc} region into the signal region.

Candidate $B_d^0 \to J/\psi K_L$ decays are selected by requiring the observed K_L direction to be within 45° from the direction expected for a two-body decay (ignoring the B_d^0 cms motion). We reduce the background by means of a likelihood quantity that depends on the J/ψ cms momentum, the angle between the K_L and its nearest-neighbor charged track, the charged track multiplicity, and the kinematics that are obtained when the event is reconstructed assuming a $B^+ \to J/\psi K^{*+}(K_L\pi^+)$ hypothesis. In addition, we remove events that are reconstructed as $B_d^0 \to J/\psi K_S$, $J/\psi K^{*0}(K^+\pi^-, K_S\pi^0)$, $B^+ \to J/\psi K^+$, or $J/\psi K^{*+}(K^+\pi^0, K_S\pi^+)$ decays. Figure 2 shows the $p_B^{\rm cms}$ distribution, calculated for a $B_d^0 \to J/\psi K_L$ two-body

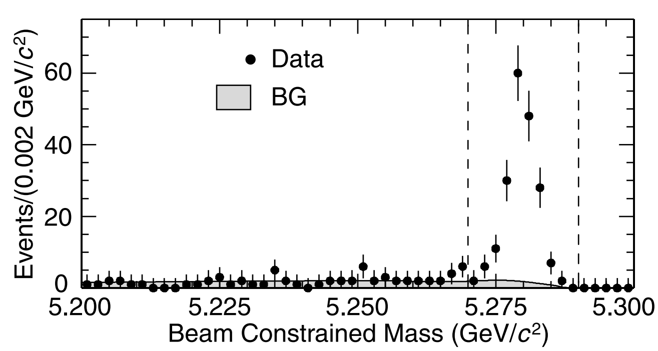

FIG. 1. The beam-constrained mass distribution for all decay modes combined (other than $B_d^0 \to J/\psi K_L$). The shaded area is the estimated background. The dashed lines indicate the signal region.

TABLE I. The numbers of CP-eigenstate events.

Mode	N_{ev}	N_{bkgd}
$J/\psi(\ell^+\ell^-)K_S(\pi^+\pi^-)$	123	3.7
$J/\psi(\ell^+\ell^-)K_S(\pi^0\pi^0)$	19	2.5
$\psi(2S)(\ell^+\ell^-)K_S(\pi^+\pi^-)$	13	0.3
$\psi(2S)(J/\psi\pi^+\pi^-)K_S(\pi^+\pi^-)$	11	0.3
$\chi_{c1}(\gamma J/\psi)K_S(\pi^+\pi^-)$	3	0.5
$\eta_c(K^+K^-\pi^0)K_S(\pi^+\pi^-)$	10	2.4
$\eta_c(K_SK^+\pi^-)K_S(\pi^+\pi^-)$	5	0.4
$J/\psi(\ell^+\ell^-)\pi^0$	10	0.9
Sub-total	194	11
$J/\psi(\ell^+\ell^-)K_L$	131	54

decay hypothesis, for the surviving events. The histograms in the figure are the results of a fit to the signal and background distributions, where the shapes are derived from Monte Carlo (MC) simulations [7], and the normalizations are allowed to vary. Among the total of 131 entries in the $0.2 \leq p_B^{\mathrm{cms}} \leq 0.45$ GeV/c signal region, the fit finds 77 $J/\psi K_L$ events.

The leptons and charged pions and kaons among the tracks which are not associated with f_{CP} are used to identify the flavor of the accompanying B meson. Tracks are selected in several categories that distinguish the b-flavor by the track's charge: high momentum leptons from $b \to c\ell^-\overline{\nu}$, lower momentum leptons from $c \to s\ell^+\nu$, charged kaons from $b \to c \to s$, high momentum pions from decays of the type $B_d^0 \to D^{(*)-}$ (π^+, ρ^+, a_1^+, etc.), and slow pions from $D^{*-} \to \overline{D}^0\pi^-$. For each track in one of these categories, we use the MC to determine the relative probability that it originates from a B_d^0 or $\overline{B}_d^0$ as a function of its charge, cms momentum and polar angle, particle-identification probability, and other kinematic and event-shape quantities. We combine the results from the different track categories (taking into account correlations for the case of multiple inputs) to determine a b-flavor q, where $q = +1$ when f_{tag} is more likely to be a B_d^0 and -1 for a

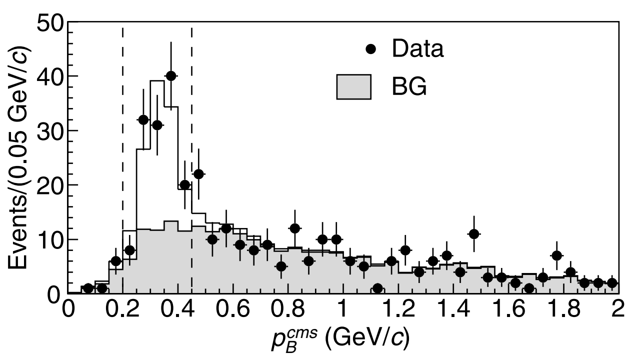

FIG. 2. The p_B^{cms} distribution for $B_d^0 \to J/\psi K_L$ candidates with the results of the fit. The solid line is the signal plus background; the shaded area is background only; the dashed lines indicate the signal region.

$\overline{B}_d^0$. We use the MC to evaluate an event-by-event flavor-tagging dilution factor, r, which ranges from $r = 0$ for no flavor discrimination to $r = 1$ for perfect flavor assignment. We use r only to categorize the event. For the CP asymmetry analysis, we use the data to correct for wrong-flavor assignments.

The probabilities for an incorrect flavor assignment, w_l ($l = 1, 6$), are measured directly from the data for six r intervals using a sample of exclusively reconstructed, self-tagged $B_d^0 \to D^{*-}\ell^+\nu$, $D^{(*)-}\pi^+$, and $D^{*-}\rho^+$ decays. The b-flavor of the accompanying B meson is assigned according to the above-described flavor-tagging algorithm, and values of w_l are determined from the amplitudes of the time-dependent B_d^0-$\overline{B}_d^0$ mixing oscillations [8]: $(N_{OF} - N_{SF})/(N_{OF} + N_{SF}) = (1 - 2w_l)\cos(\Delta m_d \Delta t)$. Here N_{OF} and N_{SF} are the numbers of opposite and same flavor events. Table II lists the resulting w_l values together with the fraction of the events (f_l) in each r interval. All events in Table I fall into one of the six r intervals. The total effective tagging efficiency is $\sum_l f_l(1 - 2w_l)^2 = 0.270^{+0.021}_{-0.022}$, where the error includes both statistical and systematic uncertainties, in good agreement with the MC result of 0.274. We check for a possible bias in the flavor tagging by measuring the effective tagging efficiency for B_d^0 and $\overline{B}_d^0$ self-tagged samples separately, and for different Δt intervals. We find no statistically significant difference.

The vertex positions for the f_{CP} and f_{tag} decays are reconstructed using tracks that have at least one three-dimensional coordinate determined from associated $r\phi$ and z hits in the same SVD layer plus one or more additional z hits in other SVD layers. Each vertex position is required to be consistent with the IP profile smeared in the $r\phi$ plane by the B-meson decay length. (The IP size, determined run-by-run, is typically $\sigma_x \simeq 100$ μm, $\sigma_y \simeq 5$ μm, and $\sigma_z \simeq 3$ mm.) The f_{CP} vertex is determined by using lepton tracks from the J/ψ or $\psi(2S)$ decays, or prompt tracks from η_c decays. The f_{tag} vertex is determined from tracks not assigned to f_{CP} with additional requirements of $\delta r < 0.5$ mm, $\delta z < 1.8$ mm, and $\sigma_{\delta z} < 0.5$ mm, where δr and δz are the distances of the closest approach to the f_{CP} vertex in the $r\phi$ plane and the z direction, respectively, and $\sigma_{\delta z}$ is the calculated error of δz. Tracks that form a K_S are removed. The MC indicates that the average z_{CP} resolution is 75 μm (rms); the z_{tag}

TABLE II. Experimentally determined event fractions (f_l) and incorrect flavor assignment probabilities (w_l) for each r interval.

l	r	f_l	w_l
1	0.000–0.250	0.393 ± 0.014	$0.470^{+0.031}_{-0.035}$
2	0.250–0.500	0.154 ± 0.007	$0.336^{+0.039}_{-0.042}$
3	0.500–0.625	0.092 ± 0.005	$0.286^{+0.037}_{-0.035}$
4	0.625–0.750	0.100 ± 0.005	$0.210^{+0.033}_{-0.031}$
5	0.750–0.875	0.121 ± 0.006	$0.098^{+0.028}_{-0.026}$
6	0.875–1.000	0.134 ± 0.006	$0.020^{+0.023}_{-0.019}$

resolution is worse (140 μm) because of the lower average momentum of the $f_{\rm tag}$ decay products and the smearing caused by secondary tracks from charmed meson decays.

The resolution function $R(\Delta t)$ for the proper time interval is parametrized as a sum of two Gaussian components: a *main* component due to the SVD vertex resolution, charmed meson lifetimes, and the effect of the cms motion of the B mesons, plus a *tail* component caused by poorly reconstructed tracks. The means ($\mu_{\rm main}$, $\mu_{\rm tail}$) and widths ($\sigma_{\rm main}$, $\sigma_{\rm tail}$) of the Gaussians are calculated event-by-event from the f_{CP} and $f_{\rm tag}$ vertex fit error matrices; average values are $\mu_{\rm main} = -0.09$ ps, $\mu_{\rm tail} = -0.78$ ps and $\sigma_{\rm main} = 1.54$ ps, $\sigma_{\rm tail} = 3.78$ ps. The negative values of the means are due to secondary tracks from charmed mesons. The relative fraction of the main Gaussian is determined to be 0.982 ± 0.013 from a study of $B_d^0 \to D^{*-}\ell^+\nu$ events. The reliability of the Δt determination and $R(\Delta t)$ parametrization is confirmed by lifetime measurements of the neutral and charged B mesons [9] which use the same procedures and are in good agreement with the world average values [10].

We determine $\sin 2\phi_1$ from an unbinned maximum-likelihood fit to the observed Δt distributions. The probability density function (pdf) expected for the signal distribution is given by

$$\mathcal{P}_{\rm sig}(\Delta t, q, w_l, \xi_f) = \frac{e^{-|\Delta t|/\tau_{B_d^0}}}{2\tau_{B_d^0}}\{1 - \xi_f q(1 - 2w_l) \times \sin 2\phi_1 \sin(\Delta m_d \Delta t)\},$$

where we fix the B_d^0 lifetime and mass difference at their world average values [10]. The pdf used for background events is $\mathcal{P}_{\rm bkg}(\Delta t) = f_\tau e^{-|\Delta t|/\tau_{\rm bkg}}/2\tau_{\rm bkg} + (1 - f_\tau)\delta(\Delta t)$, where f_τ is the fraction of the background component with an effective lifetime $\tau_{\rm bkg}$ and $\delta(\Delta t)$ is the Dirac delta function. For all f_{CP} modes, except $J/\psi K_L$, we find $f_\tau = 0.10^{+0.11}_{-0.05}$ and $\tau_{\rm bkg} = 1.75^{+1.15}_{-0.82}$ ps using events in background-dominated regions of ΔE vs M_{bc}. The $J/\psi K_L$ background is dominated by $B \to J/\psi X$ decays, where some final states are CP eigenstates and need special treatment. A MC study shows that the background contribution from the $\xi_f = -1$ sources $J/\psi K_S$, $\psi(2S)K_S$, and $\chi_{c1}K_S$ is 7.9%, while that from the $\xi_f = +1 \psi(2S)K_L$ and $\chi_{c1}K_L$ modes is 7.0%. Thus, the effects on the CP asymmetry from these states nearly cancel. The remaining dominant CP mode, $J/\psi K^*(K_L\pi^0)$, which accounts for 19% of the total background, is taken to be a 73/27 mixture of $\xi_f = -1$ and $+1$, respectively, based on our measurement of the J/ψ polarization in the $B_d^0 \to J/\psi K^{*0}(K_S\pi^0)$ decay [11]. For the $J/\psi K^*(K_L\pi^0)$ background pdf, we use $\mathcal{P}_{\rm sig}$ with effective CP eigenvalue $\xi_f = -0.46^{+1.46}_{-0.54}$, where the error has been expanded to include all possible values. For the non-CP background modes we use $\mathcal{P}_{\rm bkg}$ with $f_\tau = 1$ and $\tau_{\rm bkg} = \tau_B$.

The pdfs are convolved with $R(\Delta t)$ to determine the likelihood value for each event as a function of $\sin 2\phi_1$:

$$\mathcal{L}_i = \int \{f_{\rm sig}\mathcal{P}_{\rm sig}(\Delta t', q, w_l, \xi_f) + (1 - f_{\rm sig})\mathcal{P}_{\rm bkg}(\Delta t')\} \times R(\Delta t - \Delta t')\, d\Delta t',$$

where $f_{\rm sig}$ is the probability that the event is signal, calculated as a function of $p_B^{\rm cms}$ for $J/\psi K_L$ and of ΔE and M_{bc} for other modes. The most probable $\sin 2\phi_1$ is the value that maximizes the likelihood function $L = \prod_i \mathcal{L}_i$, where the product is over all events. We performed a blind analysis: the fitting algorithms were developed and finalized using a flavor-tagging routine that does not divulge the sign of q. The sign of q was then turned on, and the application of the fit to all of the events listed in Table I produces the result $\sin 2\phi_1 = 0.58^{+0.32+0.09}_{-0.34-0.10}$, where the first error is statistical and the second is systematic. The systematic errors are dominated by the uncertainties in w_l ($^{+0.05}_{-0.07}$) and the $J/\psi K_L$ background (± 0.05). Separate fits to the $\xi_f = -1$ and $\xi_f = +1$ event samples give $0.82^{+0.36}_{-0.41}$ and $0.10^{+0.57}_{-0.60}$, respectively [12]. Figure 3(a) shows $-2\ln(L/L_{\rm max})$ as a function of $\sin 2\phi_1$ for the $\xi_f = -1$ and $\xi_f = +1$ modes separately and for both modes combined. Figure 3(b) shows the asymmetry obtained by performing the fit to events in Δt bins separately, together with a curve that represents $\sin 2\phi_1 \sin(\Delta m_d \Delta t)$ for $\sin 2\phi_1 = 0.58$.

We check for a possible fit bias by applying the same fit to non-CP eigenstate modes: $B_d^0 \to D^{(*)-}\pi^+$, $D^{*-}\rho^+$,

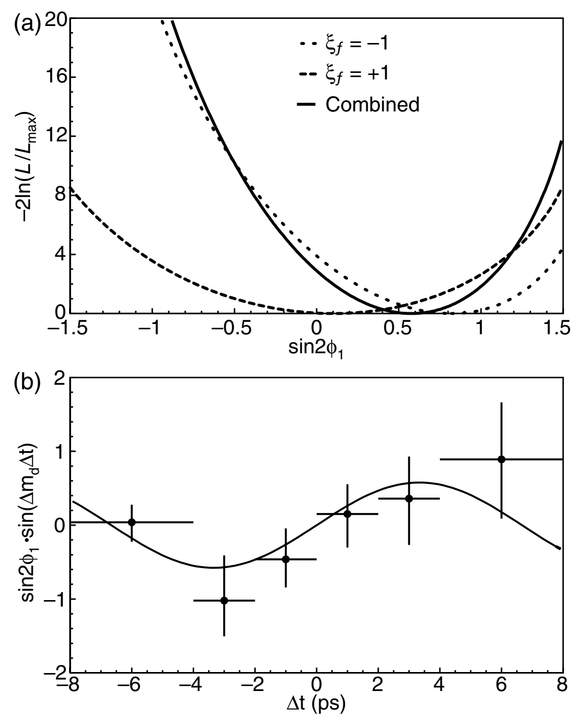

FIG. 3. (a) Values of $-2\ln(L/L_{\rm max})$ vs $\sin 2\phi_1$ for the $\xi_f = -1$ and $+1$ modes separately and for both modes combined. (b) The asymmetry obtained from separate fits to each Δt bin; the curve is the result of the global fit ($\sin 2\phi_1 = 0.58$).

$J/\psi K^{*0}(K^+\pi^-)$, and $D^{*-}\ell^+\nu$, where "$\sin 2\phi_1$" should be zero, and the charged mode $B^+ \to J/\psi K^+$. For all of the modes combined we find 0.065 ± 0.075, consistent with a null asymmetry.

We have presented a measurement of the standard model CP violation parameter $\sin 2\phi_1$ based on a 10.5 fb^{-1} data sample collected at the $\Upsilon(4S)$:

$$\sin 2\phi_1 = 0.58^{+0.32}_{-0.34}(\text{stat})^{+0.09}_{-0.10}(\text{syst}) .$$

The probability of observing $\sin 2\phi_1 > 0.58$, if the true value is zero, is 4.9%. Our measurement is more precise than the previous measurements [13] and consistent with SM constraints [14].

We wish to thank the KEKB Accelerator Group for the excellent operation. We acknowledge support from the Ministry of Education, Culture, Sports, Science and Technology of Japan and the Japan Society for the Promotion of Science; the Australian Research Council and the Australian Department of Industry, Science and Resources; the Department of Science and Technology of India; the BK21 program of the Ministry of Education of Korea and the SRC program of the Korea Science and Engineering Foundation; the Polish State Committee for Scientific Research under Contract No. 2P03B 17017; the Ministry of Science and Technology of Russian Federation; the National Science Council and the Ministry of Education of Taiwan; the Japan-Taiwan Cooperative Program of the Interchange Association; and the U.S. Department of Energy.

[1] M. Kobayashi and T. Maskawa, Prog. Theor. Phys. **49**, 652 (1973).

[2] A. B. Carter and A. I. Sanda, Phys. Rev. D **23**, 1567 (1981); I. I. Bigi and A. I. Sanda, Nucl. Phys. **B193**, 85 (1981).

[3] H. Quinn and A. I. Sanda, Eur. Phys. J. C **15**, 626 (2000). (Some papers refer to this angle as β.)

[4] Belle Collaboration, K. Abe *et al.* (to be published), KEK Report No. 2000-4.

[5] KEKB B Factory Design Report No. 95-1, 1995 (unpublished).

[6] Throughout this Letter, when a mode is quoted the inclusion of the charge conjugate mode is implied.

[7] We use the QQ B-meson decay event generator developed by the CLEO Collaboration (http://www.lns.cornell.edu/public/CLEO/soft/QQ) and GEANT3 for the detector simulation; CERN Program Library Long Writeup W5013, CERN, 1993.

[8] Belle Collaboration, J. Suzuki, Proceedings of the 30th International Conference on High Energy Physics, Osaka, 2000 (to be published).

[9] Belle Collaboration, H. Tajima, Proceedings of the 30th International Conference on High Energy Physics, Osaka, 2000 (to be published).

[10] Particle Data Group, D. E. Groom *et al.,* Eur. Phys. J. C **15**, 1 (2000).

[11] Belle Collaboration, S. Schrenk, Proceedings of the 30th International Conference on High Energy Physics, Osaka, 2000 (to be published). This result agrees within errors with those of CLEO Collaboration, C. P. Jessop *et al.* [Phys. Rev. Lett. **79**, 4533 (1997)] and CDF Collaboration, T. Affolder *et al.* [Phys. Rev. Lett. **85**, 4668 (2000)].

[12] A fit to only the $B^0_d \to J/\psi K_S(\pi^+\pi^-)$ events gives a $\sin 2\phi_1$ value of $1.21^{+0.40}_{-0.47}$; a fit to only the non-$J/\psi K_S$ $\xi = -1$ modes gives $-0.05^{+0.76}_{-0.74}$. Separate fits to the $q = +1$ and $q = -1$ event samples give $\sin 2\phi_1$ values of $0.40^{+0.47}_{-0.49}$ and $0.73^{+0.41}_{-0.46}$, respectively.

[13] OPAL Collaboration, K. Ackerstaff *et al.,* Eur. Phys. J. C **5**, 379 (1998); CDF Collaboration, T. Affolder *et al.,* Phys. Rev. D **61**, 072005 (2000); ALEPH Collaboration, R. Barate *et al.,* Phys. Lett. B **492**, 259 (2000).

[14] See, for example, S. Mele, Phys. Rev. D **59**, 113011 (1999).